Static Scattering Function for a Regular Star-Branched Polymer

J. L. Alessandrini*,† and M. A. Carignano‡

Departamento de Física, Facultad de Ciencias Exactas, Universidad Nacional de La Plata, C.C. 67, 1900 La Plata, Argentina

Received July 22, 1991; Revised Manuscript Received October 4, 1991

ABSTRACT: The static scattering function for a regular star-branched polymer is calculated in the full excluded-volume limit with renormalization group techniques, and a closed-form expression for the scattering intensity $I(k)$ is given. The influence of the excluded-volume interaction between monomers becomes more noticeable as the functionality f of the star increases, qualitative differences appearing between $I(k)$ and the Gaussian limit $I_0(k)$. A simplified formula for $I(k)$ is provided, which can be used for the treatment of experimental data. The scattering of one labeled arm of the star is also investigated and the radius of gyration of the arm is calculated, giving a quantitative expression for the stretching of the branches.

I. Introduction

Star polymers are receiving nowadays considerable attention in the literature from both experimental[1-5] and theoretical[6-13] points of view. The star-shaped polymers are the simplest branched structures in nature, and their study appears as the first step to the understanding of more complex systems such as gels and rubber. The topological constraint imposed by the presence of a seed or center molecule changes considerably the configurational and dynamical properties of the star polymers from a system of linear chains of the same molecular weight.

The theoretical treatment pioneered by Zimm and Stockmayer[14] on the random-walk model of stars of f branches was followed more recently by computer simulations[8-11] and numerical[12] and analytical developments[13] with the purpose of incorporating in a realistic way the effect of the excluded-volume interactions between monomers in good solvents. The conformational space renormalization group (RG) technique, introduced by Oono and Freed[15] to study linear polymer chains, has been applied to starlike polymers by Miyake and Freed.[13] They evaluated the distribution function for intersegment distance vectors and several averages in order to determine the configurational properties of uniform star polymers, in the asymptotic $N \to \infty$ limit, where N is the total length of the chain. Their results show some departure from the scaling blob theory[6] but agree with Monte Carlo simulations[8] for a low ($f \leq 6$) degree of branching.

Here we concentrate on the calculation of the scattering form factor of f-branched star polymers with the conformational space renormalization group method. It is related of course to the segmental density distribution function around the center of the star and is directly measured in standard elastic scattering experiments. The whole range of transfer momenta gives information about concentration fluctuations at different scales within the polymer coil. Moreover, some authors[2,5] extract the radius of gyration of the stars in good solvents from a fit of the scattering intensity with the static structure factor of regular stars with Gaussian statistics.[16] Hence, we explore in this paper the predictions of the RG theory about the full excluded-volume regime of the scattering function. We recover then some of the results obtained in ref 13 by another route, and we discuss the influence of the number of branches on the scattering of uniform stars in good solvents. The scattering of a single arm of the star is also discussed.

This paper is organized as follows: in section II we introduce the model and we give a short description of the fundamentals of the RG for completeness. The scattering function of the uniform f-branched star polymer in appropriate scaling limits is obtained in section III, and their properties are discussed in section IV. We describe finally our results on the scattering of one labeled arm, and we close the paper with a summary of our conclusions.

II. Theoretical Background

We give in this section a brief summary of the basic features of the star model and the chain conformation space renormalization group method[15] to introduce our notation.

The star polymer is represented by a continuous chain with f branches joined together by one end at a center, located at the origin of a d-dimensional coordinate system. We assume that all the branches have the same length N_0/f, N_0 being the microscopic measure of the total chain length. We adopt the minimal model for this system, described by the Edwards Hamiltonian, which is written as

$$H = \frac{1}{2}\sum_{i=1}^{f}\int_0^{N_0/f} d\tau_i \left[\frac{d\mathbf{c}(\tau_i)}{d\tau_i}\right]^2 + \frac{1}{2}v_0\sum_{i=1}^{f}\int\int_{|\tau_i-\tau_i'|\geq a}^{N_0/f} d\tau_i\, d\tau_i'\, \delta[\mathbf{c}(\tau_i)-\mathbf{c}(\tau_i')] + \frac{1}{2}v_0\sum_{i=1}^{f}\sum_{\substack{j=1\\ j\neq i}}^{f}\int\int_{|\tau_i+\tau_j|\geq a}^{N_0/f} d\tau_i\, d\tau_j\, \delta[\mathbf{c}(\tau_i)-\mathbf{c}(\tau_j)] \quad (2.1)$$

The conformation of the chain is described by a curve $\mathbf{c}(\tau)$ in d-space parametrized by the contour variable τ. On the ith branch, τ_i ($0 \leq \tau_i \leq N_0/f$) increases from the star center at position $\mathbf{c}(\tau_i=0) = 0$. (The variable $\mathbf{c}$ is related to the ordinary vector position through $\mathbf{c}(\tau_i) = (d/l)^{1/2}\mathbf{r}(\tau_i)$, where l is the Kuhn effective length.) Here v_0 is the microscopic bare excluded volume describing binary interactions between units, and the cutoff parameter length a eliminates the self-interaction of (monomer) units. In eq 2.1 we have explicitly distinguished between intra- and interbranch excluded-volume interactions, and both contributions are added to the first term that describes the chain connectivity. The above Hamiltonian describes Gaussian behavior when v_0 vanishes and is an appropriate model for the full excluded-volume case in the $v_0 N_0^{\epsilon/2} \to$

† Member of Comisión de Investigaciones Científicas de la Provincia de Buenos Aires (CIC), Argentina.

‡ Fellow of Consejo Nacional de Investigaciones Científicas y Técnicas (CONICET), Argentina.

0024-9297/92/2225-1157$03.00/0

∞ limit, where $\epsilon = 4 - d$.

The microscopic model defined by eq 2.1 can be used to calculate the bare static structure function $S_B(\mathbf{k},N_0,v_0;a)$ of a star-branched chain of length N_0, for a fixed scattering vector $\mathbf{k}$. This function, also called the coherent scattering function, is the Fourier transform of the (monomer) density correlation function and can be expressed as

$$S_B(k,N_0,v_0;a) = \sum_{i=1}^{f}\int d\tau_i \int_{|\tau_i-\tau_i'|\geq a} d\tau_i' \langle \exp[i\mathbf{k}\cdot(\mathbf{c}(\tau_i) - \mathbf{c}(\tau_i'))]\rangle + \sum_{i=1}^{f}\sum_{\substack{j=1\\ j\neq i}}^{f}\int d\tau_i \int_{|\tau_i+\tau_j|\geq a} d\tau_j \langle \exp[i\mathbf{k}\cdot(\mathbf{r}(\tau_i) - \mathbf{c}(\tau_j))]\rangle \quad (2.2)$$

where intra- and interbranch contributions are here also explicitly shown. The angular brackets denote the average over the equilibrium ensemble evaluated with the model Hamiltonian.

From the calculations on the linear chain system ($f = 1$), we know[17] that singularities appear in $S_B(k,N_0,v_0;a)$ at $\epsilon = 0$ (four dimensions) in the $a \to 0$ limit, demonstrating the strong dependence of S_B on short-wavelength microscopic details, calling for a renormalization procedure. The aim of the renormalization group method is precisely to provide a phenomenological long-wavelength-scale description of polymer systems from a microscopic model Hamiltonian. Hence, macroscopic parameters N, v, and L are introduced to designate the length of the real chain, the quality of the solvent, and a phenomenological scale length, respectively, with $L \gg a$. The number of branches f is a fixed quantity in both microscopic and macroscopic descriptions and does not need renormalization.

The observable structure function S, expressed in terms of N, v, and L, must be proportional to S_B since they are both proportional to the measurable scattered radiation intensity. It is convenient at this point to introduce the dimensionless variables

$$u_0 = v_0 L^{\epsilon/2}, \quad u = vL^{\epsilon/2} \quad (2.3)$$

The following relation between macroscopic and microscopic quantities is proposed:[17]

$$N = Z_2 N_0 \quad (2.4a)$$

$$u = u(u_0, a/L) \quad (2.4b)$$

$$S(k,N,u;L) = \lim_{a/L\to 0} Z_S^{-1} S_B(k,N_0,u_0;a) \quad (2.4c)$$

The relation $u = u(u_0)$ and the renormalizations constants Z_2 and Z_S are chosen to absorb the singularities induced in the limit $a/L \to 0$ on the right-hand side of eq 2.4c. Hence, a finite well-defined functional form $S(k,N,u;L)$ may be obtained.

A renormalization group equation for $S(k,N,u;L)$ can be written, and, at the fixed point u^*—defined as $\beta(u^*) = 0$, where $\beta(u)$ is the Gell-Mann–Low function $\beta(u) = L[\partial u/\partial L]_{a,v_0,N_0}$[17]—the scattering function satisfies a scaling law

$$S(k,N) = [N/f]^{(2+C)/(B-1)} F_f(k[N/f]^{(1-B)/2}) \quad (2.5)$$

where

$$B = L\left(\frac{\partial \ln Z_S}{\partial L}\right)_{u=u^*}$$

$$C = L\left(\frac{\partial \ln Z_2}{\partial L}\right)_{u=u^*} \quad (2.6)$$

The macroscopic scale length L was chosen as unity in the above expressions, as was done in the linear case also.[15] The unknown scaling functions F_f will be determined in the next section.

III. Calculation of the Scattering Function

The calculation of the bare scattering function S_B can be performed only in the frame of perturbation theory and is generally displayed as a double series expansion in powers of v_0 and ϵ as

$$S_B = \sum_{m,n\geq 0} S_{m,n}^{\circ} u_0^{\,m} \epsilon^n \quad (3.1)$$

where the coefficients $S_{m,n}^{\circ}$ are evaluated at four dimensions. The singularities mentioned in section II are to be eliminated order by order to make the coefficients $S_{m,n}$ of the series

$$S = \sum_{m,n\geq 0} S_{m,n}^{\circ} u^m \epsilon^n \quad (3.2)$$

well behaved in the limit $a/L \to 0$. Since the value of the dimensionless coupling constant u at the excluded-volume fixed point is $u^* \simeq O(\epsilon)$,[15] only two coefficients $S_{0,0}$ and $S_{1,0}$ are necessary for the calculation of S_B to first order in ϵ.

The calculation of the zeroth-order term is straightforward. It consists of two terms: the first one describes the scattering produced by pairs of monomers located on one of the f branches and the second one is that produced from units belonging to two of any of the $f(f-1)/2$ pairs of branches:

$$S_{0,0}^{\circ}(k,N_0) = f\int_0^{N_0/f} d\tau \int_0^{N_0/f} d\sigma \exp(-|\tau - \sigma|k^2/2) + f(f-1)\int_0^{N_0/f} d\tau \int_0^{N_0/f} d\sigma \exp(-|\tau + \sigma|k^2/2) = N_0^2 f(\varphi_0) \quad (3.3)$$

where

$$f(\varphi_0) = \frac{1}{f}P(\varphi_0) + \frac{f-1}{f}Q^2(\varphi_0) \quad (3.4)$$

and

$$P(\varphi_0) = 2\left[\frac{e^{-\varphi_0}}{\varphi_0^2} - \frac{1}{\varphi_0^2} + \frac{1}{\varphi_0}\right]$$

$$Q(\varphi_0) = \frac{e^{-\varphi_0} - 1}{\varphi_0} \quad (3.5)$$

and $\varphi_0 = N_0 k^2/2f$. Equation 3.3 is known in the literature as the Benoit function[16] and describes the scattering by star polymers whose arms satisfy random Gaussian statistics. Moreover, it is independent of the dimension of the space.

Following the procedure of ref 17, we present our first-order calculations in a diagrammatic fashion. Diagrams are generated when the Boltzmann factor $\exp(-H)$ is expanded in powers of u_0 and replaced in the definition of S_B, eq 2.2. We get the following expression

$$S_B(k,N_0,u_0;a) = S_{0,0}^{\circ}(k,N_0) + u_0 S_{1,0}^{\circ}(k,N_0;a) \quad (3.6)$$

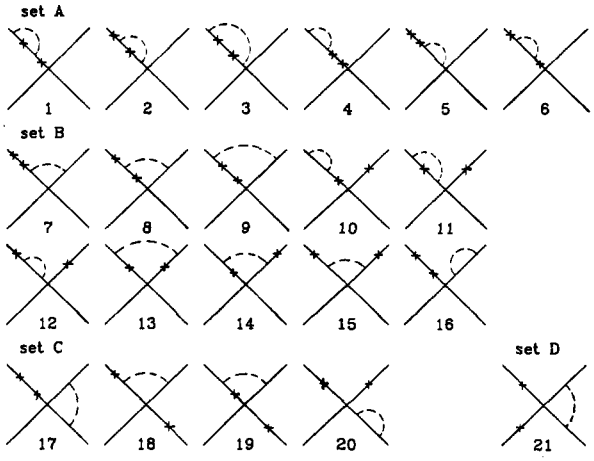

Figure 1. Diagrammatic representation of the first-order contribution to $S(k)$. Set A contains diagrams identical to those of the linear chain. Sets B–D involve more than one arm in the labeling process with crosses (k insertions) or points (interactions).

with

$$S_{1,0}^{\circ}(k,N_0;a) = \sum_{i=1}^{21} w(f)\ \sigma_i U_i(k,N_0;a) \tag{3.7}$$

where $w(f)$ are weights associated to sets of diagrams, σ_i are appropriate symmetry factors, and U_i is the contribution of the ith diagram.

There is a total of 21 diagrams to first order in u_0; they are collected in Figure 1 and are classified in four sets (A–D), according to the number of branches involved in the labeling process with crosses (k insertions) or points (interactions). Each set has an associate weight w (equal to f, $f(f-1)$, $f(f-1)(f-2)$, and $f(f-1)(f-2)(f-3)$, for sets A–D, respectively), and the majority of the symmetry factors σ_i are unity. Exceptions are $\sigma_{13} = \sigma_{15} = {}^1/_2$ (set B), $\sigma_{17} = \sigma_{20} = {}^1/_2$ (set C), and $\sigma_{21} = {}^1/_4$ (set D).

All the diagrams were evaluated at $\epsilon = 0$, and a short contour distance cutoff a was retained on otherwise divergent contributions in the $a \to 0$ limit. The result of the calculation of each diagram is written as $U_i = U_i^{S} + U_i^{R}$, where the superscript S (R) means the singular (regular) contributions.

The resulting singular part $S_{0,1}^{\circ}|_S$ of the first-order coefficient $S_{0,1}^{\circ}$ was obtained as

$$S_{0,1}^{\circ}|_S(k,N_0;a) = \frac{-N_0^2}{4\pi^2}\Big\{[P(\varphi_0) + (f-1)Q(\varphi_0)]\frac{N_0}{fa} + \frac{1}{f^2}\Big(w_A[P(\varphi_0) + 2Q(\varphi_0)] + w_B[2Q(\varphi_0)e^{-\varphi_0} + Q^2(\varphi_0)] + w_C[P(\varphi_0)/2 + Q^2(\varphi_0)] + w_D Q^2(\varphi_0)/2\Big)\ln\frac{N_0}{fa}\Big\} \tag{3.8}$$

while the contribution of the regular part is given by

$$S_{0,1}^{\circ}|_R(k,N_0) = \frac{N_0^2}{4\pi^2}g(\varphi_0) \tag{3.9}$$

(The individual contributions to the function $g(\varphi_0)$ are listed in the appendix.) The singular terms linear in N_0/af may be eliminated by adopting a first-order normalization of the partition function:

$$Z(N_0,u_0;a) = 1 - \frac{u_0}{4\pi^2}f\Big[\frac{N_0}{fa} + \frac{f-3}{2}\ln\frac{N_0}{fa} - 1 - \frac{f-1}{2}\ln 2\Big] \tag{3.10}$$

Hence, the bare scattering function reads

$$S_B(k,N_0,u_0;a) = N_0^2\Big\{f(\varphi_0) + \frac{u_0}{4\pi^2}\Big(g(\varphi_0) - \Big[f + \frac{f(f-1)\ln 2}{2}\Big]f(\varphi_0)\Big) + \frac{u_0}{4\pi^2}(f^2 - 3f + 1)f(\varphi_0)\ln\frac{N_0}{fa}\Big\} \tag{3.11}$$

If we choose the renormalization constants Z_2 and Z_S as

$$Z_2 = 1 + \frac{u}{4\pi^2}\ln\frac{L}{a}$$

$$Z_S = 1 - 2\frac{u}{4\pi^2}\ln\frac{L}{a} \tag{3.12}$$

the remaining logarithmic singularities as $a \to 0$ are eliminated in the right-hand side of eq 2.4c and we get

$$S(k,N,u;L) = N^2\Big\{f(\beta) + \frac{u}{4\pi^2}\beta f'(\beta)\ln\frac{N}{fL} + \frac{u}{4\pi^2}\Big(g(\beta) - \Big[f + \frac{f(f-1)\ln 2}{2}\Big]f(\beta)\Big)\Big\} \tag{3.13}$$

where the auxiliary variable $\beta = Nk^2/2f$ was introduced.

The self-avoiding critical point is found to be independent of the topology of the chain[13,18] and reads

$$u^* = \frac{\epsilon}{2}\pi^2 + O(\epsilon^2) \tag{3.14}$$

Introducing now the scaling variable φ

$$\varphi = \beta\Big[1 + \frac{\epsilon}{8}\ln\frac{N}{fL}\Big] \simeq \beta\Big[\frac{N}{fL}\Big]^{\epsilon/8} \tag{3.15}$$

the renormalized scattering structure function is written, finally, as

$$S(k,N) = N^2 f(\varphi)\exp\Big\{-\frac{\epsilon}{8}\Big[f + \frac{f(f-1)\ln 2}{2} - \frac{g(\varphi)}{f(\varphi)}\Big]\Big\} \tag{3.16}$$

This expression generalizes the well-known result for linear chains. Comparing it with eq 2.5, we obtain both the scaling function $F_f(x)$ and the quantities $B = \epsilon/8$ and $C = -\epsilon/4$.

IV. Properties of the Scattering Function

Introducing the $k = 0$ limit of eq 3.16, we get for the scattering intensity $I(k,N)$

$$I(k,N) \equiv \frac{S(k,N)}{S(0,N)} = f(\varphi)\exp\Big\{\frac{\epsilon}{8}\Big[\frac{g(\varphi)}{f(\varphi)} - \frac{g(0)}{f(0)}\Big]\Big\} \tag{4.1}$$

whose small-k expansion in d space gives information about the mean-squared radius of gyration $\langle S^2\rangle$, named R_g^2 in the following:

$$I(k,N) = 1 - \frac{k^2R_g^2}{d} + \ldots \tag{4.2}$$

Expanding eq 4.1 in powers of φ and comparing with eq 4.2, we get

$$R_g^2 = \frac{dN}{6}\Big[\frac{N}{fL}\Big]^{\epsilon/8}\frac{3f-2}{f^2}\Big\{1 + \frac{\epsilon}{8}\Big[\frac{1}{2-3f}\Big(\frac{13}{2}(f-1)(f-2) - 4(f-1)(3f-5)\ln 2\Big) - \frac{13}{12}\Big]\Big\} \tag{4.3}$$

Dividing the above result with that corresponding to $f =$

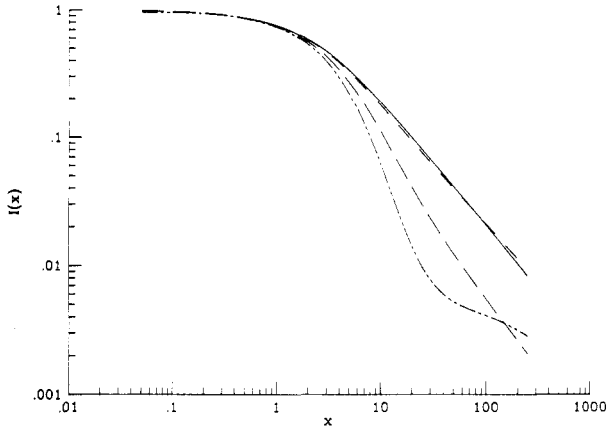

Figure 2. Comparison of the scattering intensity $I(x)$ at both Gaussian (G) and self-avoiding (SA) fixed points for linear and 12-arm regular star polymers ($d = 3$). Linear chain: solid line (G), short dashed line (SA). 12-arm star: long dashed line (G), dotted–dashed line (SA).

1 (linear chain), we finally get the so-called g factor[1-5]

$$g(f) = \frac{R_g^2}{R_g^2(f=1)} = \frac{3f-2}{f^2}\left\{1 + \frac{\epsilon}{8}\left[\frac{1}{2-3f}\left(\frac{13}{2}(f-1)(f-2) - 4(f-1)(3f-5)\ln 2\right)\right]\right\} \quad (4.4)$$

This quantity agrees with that obtained by Miyake and Freed in their analysis of the distribution function of internal distances.[19]

Instead of using the scaling variable φ, it is useful to display the results in terms of a dimensionless variable y proportional to $x = k^2R_g^2$, defined by

$$y = \frac{3}{4}\left[\frac{f}{3f-2}\right]x = [1 - \epsilon/4][1 - C_f\epsilon]\varphi \quad (4.5)$$

where the coefficients C_f are evaluated from the knowledge of the functions $f(\varphi)$, $g(\varphi)$, and their derivatives at the origin

$$C_f = \frac{1}{8}\left[\frac{g(0)}{f(0)} - \frac{g'(0)}{f'(0)}\right] \quad (4.6)$$

The behavior of C_f as a function of the number of branches is approximately represented by a linear function $C_f \cong 0.2 - 0.076f$. It is seen that the error introduced by the above replacement is minimal for $f \cong 6$. Then the scattering intensity reads

$$I(y) = f(y)\exp\left\{\frac{\epsilon f'(y)}{4f(y)}y\right\}\exp\left\{\epsilon C_f\frac{f'(y)}{f(y)}y\right\}\times \exp\left\{\frac{\epsilon}{8}\left[\frac{g(y)}{f(y)} - \frac{g(0)}{f(0)}\right]\right\} \quad (4.7)$$

For comparison, we plotted in Figure 2 the scattering intensities in three dimensions for linear and 12-arm star polymers both at random Gaussian and full excluded-volume fixed points, denoted by $I_0(x)$ and $I(x)$, respectively. The former was obtained from the Benoit function, eq 3.3. Even if in the linear polymer case[17] one can hardly distinguish $I(x)$ from $I_0(x)$, noticeable differences arise for higher functionalities in the logarithmic representation.

It is customary to analyze the scattering data with the Kratky plot, where $xI(x)$ vs $x^{1/2}$ is plotted. In Figure 3 we show our results for functionalities $f = 1$, 5, 12, and 18 in the SAW limit. The corresponding predictions from

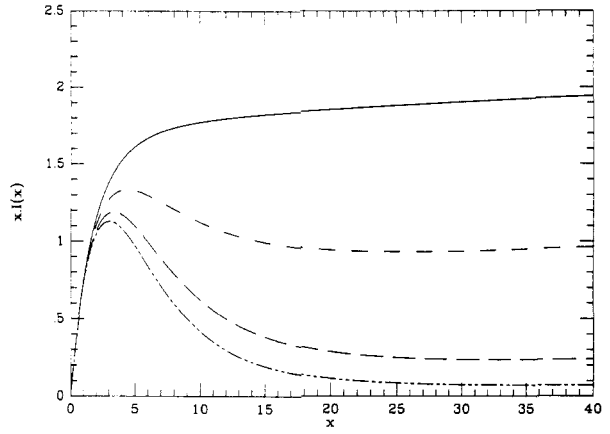

Figure 3. Kratky plot for regular star polymers of different functionalities at the SA fixed point: solid line, $f = 1$; short dashed line, $f = 5$; long dashed line, $f = 12$; dotted-dashed line, $f = 18$.

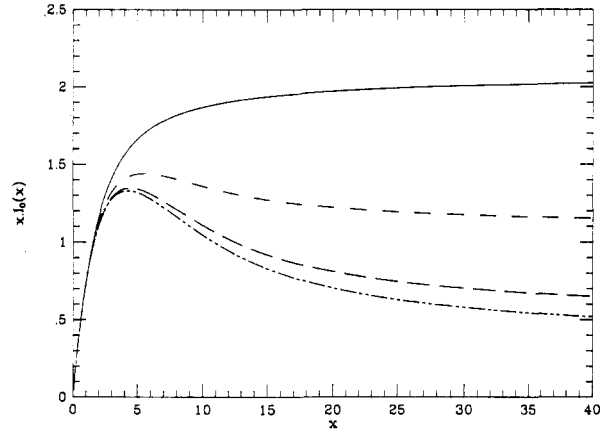

Figure 4. Same as in Figure 3, at the Gaussian fixed point.

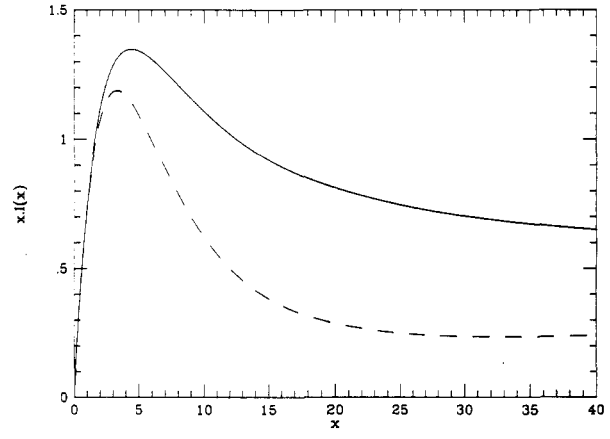

Figure 5. Kratky plot for 12-arm regular stars at Gaussian (solid line) and SA (dashed line) fixed points.

random Gaussian chains are displayed in Figure 4. Except for the linear case, a maximum at intermediate values of $x^{1/2}$ is shown by star polymers. The width of the "shape line" is smaller when the number of arms increases and, at fixed f, decreases with excluded-volume effects. For comparison, the data for $f = 12$ are reproduced in Figure 5 in the two limiting cases.[19]

In the high-k limit, scaling arguments predict that the scattering intensity behaves as[20]

$$I(x) \sim x^{-1/\nu} \quad (4.8)$$

independent of the chain length. Here ν is the size exponent relating the mean-squared radius of gyration of a polymer chain to its total contour length N: $R_g^2 \sim N^{2\nu}$.

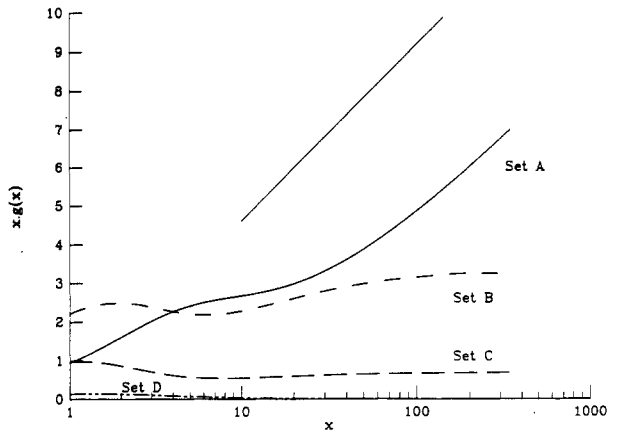

Figure 6. Contribution of the different sets of diagrams to $x|g(x)|$. The straight line represents the expected asymptotic behavior (eq 4.10). Only the linear polymer diagrams (set A) are relevant to this scaling limit.

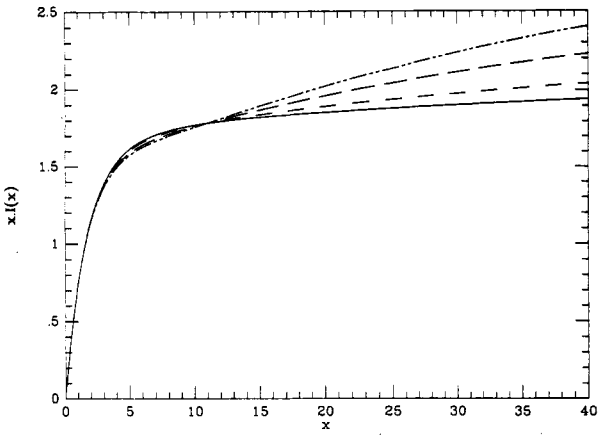

Figure 7. Kratky plot for the one-arm scattering intensity $I(x)$ at the SA fixed point for different functionalities (f = 1, 5, 12, 18). Same labels as in Figure 3.

For Gaussian chains, $\nu = 1/2$ and a plateau is reached in the Kratky representation. SAW chains show, instead, an upturn effect with constant slope compatible with the excluded-volume exponent to $O(\epsilon)$:[20]

$$\nu = \frac{1}{2}\left[1 + \frac{\epsilon}{8} + ...\right] \tag{4.9}$$

An inspection of eq 4.1 shows that, in order that eq 4.8 be satisfied, the asymptotic behavior of $g(x)$ must be

$$x|g(x)| \sim 2 \ln x \tag{4.10}$$

In Figure 6 we plotted separately the large-x behavior of the contributions of the different sets of diagrams to $x|g(x)|$. It is seen that only set A displays the expected limit; all other contributions either achieve a plateau or decrease to zero. Clearly, not all the diagrams within a given set behave in a similar way, as noted for the linear case in ref 17, but the global tendency is that only excluded volume within each arm dominates this asymptotic limit. This effect may be interpreted as due to a kind of screening of the excluded volume between monomers located on different arms at small scales. This screening is created by the topological constraint imposed by the presence of the center of the star between any two branches.

V. One-Arm Scattering

The analysis reproduced above for the scattering of the whole branched chain can be repeated for a similar system with one labeled arm, with identical inter- and intramolecular interactions. Hence, the scattering produced by only one arm of the star may be studied as is done in elastic and quasielastic neutron scattering experiments.[3]

The details of the calculations will not be reproduced here. The perturbation method is straightforward, and only a selected set of diagrams contributes to the one-arm scattering function. They are diagrams U_1–U_6 from set A (linear chain diagrams), U_7–U_9 and U_{16} (set B), and U_{17} (set C), since they have altogether the two k insertions on the same arm. The factor f is to be eliminated from the original weights of those diagrams since the labeling process destroys the identity of the f arms. The renormalization constants Z_2 and Z_S are again given by eq 3.12. The one-arm scattering intensity preserves the functional form of that of the star chain eqs 4.1 and 4.7, with functions $f(\varphi) = P(\varphi)$ and $g(\varphi)$ corresponding to one labeled arm. The resulting one-arm mean-squared radius of gyration R_g^2(one arm) reads

$$R_g^2 = \frac{dN}{6f}\left(\frac{N}{fL}\right)^{\epsilon/8}\left\{1 - \epsilon\left[\frac{13}{96} - (f-1)\left(\frac{35}{64} - \frac{3}{4}\ln 2\right)\right]\right\} \tag{5.1}$$

Taking the ratio of this quantity to that of the mean-squared radius of gyration for a single linear chain with total length N/f, we get an analytical expression for the stretching of one arm induced by excluded-volume effects of the remaining $f - 1$ arms:

$$j = 1 + \epsilon(f-1)\left[\frac{35}{64} - \frac{3}{4}\ln 2\right] \tag{5.2}$$

The scattering intensity I(one arm) of a single labeled arm of the star molecule is essentially that of the linear chain. At the Gaussian fixed point, it is exactly the Debye function, as expected. Differences arise at the SAW fixed point. Even if its asymptotic behavior is dominated by the one-arm diagrams (set A), the influence of the weights associated to them makes that the asymptotic limit is achieved at lower values of the adimensional variable $y = (3/4)k^2R_g^2$(one arm) as f increases. This behavior is displayed in Figure 7. It is evident from that Kratky plot that the one-arm scattering law at high k values strongly depends on the functionality of the star.

VI. Discussion

The influence of the excluded-volume effect on the scattering function of flexible polymer chains is (clearly) noticeable in those systems with topology other than that of the linear ones. In this paper, we fully analyzed regular starlike polymers. Our results are summarized in the previous sections, and we introduce here a simple formula to account for the elastic scattering in the extreme self-avoiding walk limit.

The best nonlinear fit of eq 4.7 with standard routines gives

$$I(y) = f(y)\{1 + A_1[e^{-A_2 y} - 1] + A_3 y + A_4 y^2\} \tag{6.1}$$

where the dependence of the coefficients $A_1, ..., A_4$ on the functionality f is depicted in Table I.

It is worth noting that the experimental values of $I(k)$ in good solvents are currently fitted by a Benoit function with a variable parameter, namely, the value of the R_g^2 (included in the definition of the variable y, eq 4.5), times a multiplicative constant independent of k.[2,5] Our theoretical results do not support this procedure. In fact, the shape lines at both fixed points are definitively different (even qualitatively) from each other. Figure 5 illustrates the strong discrepancy of the full width at half-maximum

Table I
Coefficients of the Best Nonlinear Fit (Equation 6.1) for the Scattering Intensity $I(y)$ and Different Functionalities, As Explained in the Text

f	A_1	A_2	A_3	A_4
1	0.27	0.31	8×10^{-4}	4×10^{-7}
5	0.55	0.48	0.019	-2×10^{-4}
12	1.0	0.36	0.028	-2×10^{-4}
18	1.1	0.41	0.015	-2×10^{-5}

for the case $f = 12$. We propose as an alternative procedure the extraction of the radius of gyration from a fit of experimental points with our eq 6.1.

One wonders about the influence of the ϵ expansion in our results when applied to $d = 3$ dimensions. At the Gaussian fixed point ($u^* = 0$), the renormalized scattering intensity reads

$$I_0(y) = \mathrm{f}(y) \exp\left\{\frac{\epsilon \mathrm{f}'(y)}{4\mathrm{f}(y)} y\right\} \tag{6.2}$$

where f(y) is proportional to the Benoit function. From comparison with the "exact" result at $d = 3$,[16] we verify that (a) the position of the maximum observed on the Kratky plot is unchanged even up to $f = 18$ and (b) the approximation (6.2) exceeds the exact one in less than 5% for $x \geq 1$. Hence, we hope that similar errors may be present also at the full excluded-volume limit.

Concerning our one-arm scattering results, we get for the first time an explicit expression for the mean-squared radius of gyration of one arm and the related ratio (eqs 5.1 and 5.2), which put forward the influence of the functionality f on those quantities, within the limitations of the ϵ expansion in the frame of the renormalization group method.

Acknowledgment. This work was partially supported by CONICET (Argentina) under PID No. 3-056500/88.

Appendix

The regular part of each diagram U_i is denoted in the following g_i ($i = 1, 2, ..., 21$). The function $g(\varphi)$—defined by eq 3.9—is obtained from the individual contributions g_i comparing it with the eq 3.7.

set A

$$g_1(\varphi) = g_2(\varphi) = -2\left\{\frac{2}{\varphi}\int_0^1 dx \int_0^{x/2} dy \frac{e^{-\varphi x/4}}{x} e^{\varphi y^2/x} + \left(\frac{1}{\varphi} - \frac{1}{\varphi^2}\right)\int_0^1 dx \frac{e^{-\varphi x/4} - 1}{x} + \frac{e^{-\varphi}}{\varphi^2}\int_0^1 dx \frac{e^{3\varphi x/4} - 1}{x} + 2\int_0^1 dx \int_0^{x/2} dy \left(\frac{1}{\varphi} - \frac{1}{\varphi^2} + \frac{e^{-\varphi(1-x)}}{\varphi^2}\right)\frac{e^{-\varphi x/4}}{x^2}[e^{\varphi y^2/x} - 1]\right\}$$

$$g_3(\varphi) = -2\int_0^1 dx \int_0^{x/2} dy \left(\frac{1}{x} - 1\right) e^{-\varphi x/4} e^{\varphi y^2/x}$$

$$g_4(\varphi) = g_5(\varphi) = \frac{-2}{\varphi}\left\{\frac{e^{-\varphi}}{\varphi^2} - \frac{1}{\varphi^2} + \frac{1}{\varphi} - \frac{e^{-\varphi}}{\varphi^2}\int_0^1 dx \frac{e^{\varphi x} - 1 - \varphi x}{x^2}\right\}$$

$$g_6(\varphi) = -2\left\{\frac{2}{\varphi^3} - \frac{1}{\varphi^2} - \frac{e^{-\varphi}}{\varphi^2} - \frac{2e^{-\varphi}}{\varphi^3} + \left(\frac{2e^{-\varphi}}{\varphi^3} + \frac{e^{-\varphi}}{\varphi^2}\right)\int_0^1 dx \frac{e^{\varphi x} - 1 - \varphi x}{x^2} - \frac{e^{-\varphi}}{\varphi^2}\int_0^1 dx \frac{e^{\varphi x} - 1}{x}\right\}$$

set B

$$g_7(\varphi) = 2\left\{\left(\frac{2}{\varphi} - \frac{1}{\varphi^2}\right)\ln 2 - \frac{e^{-\varphi}}{\varphi^2}\int_0^1 dx \frac{e^{\varphi x} - 1}{x} + \frac{e^{-2\varphi}}{\varphi^2}\int_1^2 dx \frac{e^{\varphi x}}{x}\right\}$$

$$g_8(\varphi) = 2\left\{-\frac{1}{\varphi}\ln 2 + \frac{e^{-2\varphi}}{\varphi}\int_1^2 dx \frac{e^{\varphi x}}{x} + \frac{1}{\varphi^2}\int_0^1 dx \int_x^1 dy \times (e^{-\varphi(1-y)} - 1)\frac{e^{\varphi(x^2/y - x)} - 1 - \varphi(x^2/y - x)}{x^2} - \frac{1}{\varphi^2}\int_0^1 dx \int_{1+x}^2 dy\, (e^{-\varphi(2-y)} - 1)\frac{e^{\varphi(x^2/y-x)} - 1 - \varphi(x^2/y - x)}{x^2}\right\}$$

$$g_9(\varphi) = 2\left\{\ln 2 - \frac{3}{2} - \frac{1}{\varphi}\int_0^1 dx \int_0^1 dy \frac{e^{\varphi([y^2/(1+x)]-y)} - 1}{y} + \frac{1}{\varphi}\int_0^1 dx \int_0^1 dy \frac{e^{\varphi([y^2/(1+x)]-y)} - 1 - \varphi\left(\frac{y^2}{1+x} - y\right)}{y^2} - \frac{1}{\varphi}\int_0^1 dx \int_0^1 dy \int_0^{1-y} dz \frac{e^{-\varphi[(x+y)z/(x+y+z)]} - 1 + \varphi\frac{(x+y)z}{x+y+z}}{z^2}\right\}$$

$$g_{10}(\varphi) = 2\frac{e^{-\varphi} - 1}{\varphi}\left\{\frac{e^{-\varphi}}{\varphi^2}\int_0^1 dx \frac{e^{\varphi x} - 1 - \varphi x}{x^2} - \left(\frac{e^{-\varphi}}{\varphi^2} - \frac{1}{\varphi^2} + \frac{1}{\varphi}\right)\right\}$$

$$g_{11}(\varphi) = 2\frac{e^{-\varphi} - 1}{\varphi^2}\left\{e^{-\varphi}\int_0^1 dx \int_x^1 dy \left(\frac{1 - e^{\varphi y}}{y^2}\right) - \int_0^1 dx \int_x^1 dy\, (e^{-\varphi(1-y)} - 1)\frac{e^{\varphi(x^2/y-x)} - 1}{y^2}\right\}$$

$$g_{12}(\varphi) = 2\frac{e^{-\varphi} - 1}{\varphi^2}\left\{-\frac{1}{\varphi} + e^{-\varphi}\int_0^1 dx \frac{e^{\varphi x} - 1}{x} - e^{-\varphi}\left(\frac{1}{\varphi} + 1\right)\left(1 - \int_0^1 dx \frac{e^{\varphi x} - 1 - \varphi x}{x^2}\right)\right\}$$

$$g_{13}(\varphi) = \frac{2}{\varphi}\left\{\int_0^1 dx \int_0^{1-x} dy \int_0^{1+x} dz \frac{e^{\varphi([z^2/(x+y+1)]-z)} - 1}{z^2} - \int_0^1 dx \int_0^{1-x} dy \int_0^{1+x} dz \frac{e^{-\varphi(xy/(x+y))} - 1}{z^2}\right\}$$

$$g_{14}(\varphi) = \frac{2}{\varphi^2}\left\{-\varphi\ln 2 - \varphi e^{-2\varphi}\int_1^2 dx \frac{e^{\varphi x}}{x} + \varphi e^{-2\varphi}\int_1^2 dx\, e^{\varphi x}\ln x - \varphi e^{-\varphi}\int_0^1 dx\, e^{\varphi x}\ln x - \int_1^2 dx \int_{x-1}^x dy\, (e^{-\varphi(2-x)} - 1)\frac{e^{\varphi(y^2/x - y)} - 1 - \varphi(y^2/x - y)}{y^2}\right\}$$

$$g_{15}(\varphi) = 2\left\{\frac{e^{-2\varphi}}{\varphi}\left(\frac{1}{\varphi} - 2\right)\ln 2 + \frac{\ln 2}{\varphi^2} - \frac{e^{-2\varphi}}{\varphi^2}\int_0^1 dx \int_x^{1+x} dy \frac{e^{\varphi y} - 1 - \varphi y}{y^2} + 2\frac{e^{-\varphi}}{\varphi^2}\int_0^1 dx \frac{e^{\varphi x} - 1}{x} - 2\frac{e^{-2\varphi}}{\varphi^2}\int_1^2 dx \frac{e^{\varphi x}}{x}\right\}$$

$$g_{16}(\varphi) = 2\left(\frac{e^{-\varphi}}{\varphi^2} - \frac{1}{\varphi^2} + \frac{1}{\varphi}\right)$$

set C

$$g_{17}(\varphi) = 2 \ln 2\left(\frac{e^{-\varphi}}{\varphi^2} - \frac{1}{\varphi^2} + \frac{1}{\varphi}\right)$$

$$g_{18}(\varphi) = 2\frac{e^{-\varphi}-1}{\varphi^2}\left\{\frac{e^{-\varphi}}{\varphi}\int_0^1 dx\,\frac{e^{\varphi(x^2/(1+x))}-1}{x^2} - \frac{e^{-\varphi}}{\varphi}\int_0^1 dx\,\frac{e^{\varphi x}-1-\varphi x}{x^2} - \ln 2 - \frac{1}{\varphi}\int_0^1 dx\,\frac{e^{-\varphi(x/(1+x))}-1+\varphi\left(\frac{x}{1+x}\right)}{x^2}\right\}$$

$$g_{19}(\varphi) = 2\frac{e^{-\varphi}-1}{\varphi^2}\left\{\int_0^1 dx\int_x^1 dy\,\frac{e^{\varphi(x^2/y-x)}-1-\varphi(x^2/y-x)}{x^2} + \varphi \ln 2 - \int_0^1 dx\int_{1+x}^2 dy\,\frac{e^{\varphi(x^2/y-x)}-1-\varphi(x^2/y-x)}{x^2}\right\}$$

$$g_{20}(\varphi) = 2\frac{(e^{-\varphi}-1)^2}{\varphi^2}$$

set D

$$g_{21}(\varphi) = 2 \ln 2\frac{(e^{-\varphi}-1)^2}{\varphi^2}$$

References and Notes

(1) Huber, K.; Burchard, W.; Fetters, L. J. *Macromolecules* **1984**, *17*, 541.

(2) Richter, D.; Stühn, B.; Ewen, B.; Nerger, D. *Phys. Rev. Lett.* **1987**, *58*, 2462.

(3) Richter, D.; Farago, B.; Huang, J. S.; Fetters, L. J.; Ewen, B. *Macromolecules* **1989**, *22*, 468.

(4) Bauer, B.; Fetters, L. J.; Graessley, W.; Hadjichristidis, N.; Quack, G. *Macromolecules* **1989**, *22*, 2337.

(5) Boothroyd, A. T.; Squires, G. L.; Fetters, L. J.; Rennie, A. R.; Horton, J. C.; de Vallera, A. M. B. G. *Macromolecules* **1989**, *22*, 3130.

(6) Daoud, M.; Cotton, J. P. *J. Phys. (Les Ulis, Fr.)* **1982**, *43*, 531.

(7) Burchard, W. *Adv. Polym. Sci.* **1983**, *48*, 1.

(8) Whittington, S. G.; Lipson, J. E. G.; Wilkinson, M. K.; Gaunt, D. S. *Macromolecules* **1986**, *19*, 1241.

(9) Freire, J. J.; Pla, J.; Rey, A.; Prats, R. *Macromolecules* **1986**, *19*, 452. Freire, J. J.; Rey, A.; Garcia de la Torre, J. *Macromolecules* **1986**, *19*, 457.

(10) Grest, G.; Kremer, K.; Witten, T. A. *Macromolecules* **1987**, *20*, 1316.

(11) Batoulis, J.; Kremer, K. *Macromolecules* **1989**, *22*, 4277.

(12) Croxton, C. *Macromolecules* **1988**, *21*, 2269.

(13) Miyake, A.; Freed, K. F. *Macromolecules* **1983**, *16*, 1228. Miyake, A.; Freed, K. F. *Macromolecules* **1984**, *17*, 678.

(14) Zimm, B. H.; Stockmayer, W. H. *J. Chem. Phys.* **1949**, *17*, 1301.

(15) Oono, Y. *Adv. Chem. Phys.* **1985**, *61*, 301. Freed, K. F. *Renormalization Group Theory of Macromolecules*; Wiley-Interscience: New York, 1987.

(16) Benoit, H. *J. Polym. Sci.* **1953**, *9*, 507.

(17) Ohta, T.; Oono, Y.; Freed, K. F. *Phys. Rev.* **1982**, *A25*, 2801.

(18) Lipkin, M.; Oono, Y.; Freed, K. F. *Macromolecules* **1981**, *14*, 1270.

(19) The RG model is expected to be appropriate for a low degree of branching since the original Hamiltonian is inadequate to describe the hard-core packing at the center of the star. Our results for $f = 12$ and first order in ϵ display the expected behavior of self-avoiding stars. A detailed analysis of the core and shell scattering of the labeled stars that gives insight on the local density fluctuations will be reported elsewhere.

(20) de Gennes, P.-G. *Scaling Concepts in Polymers Physics*; Cornell University Press: Ithaca, NY, 1979.